HYDRO-DYNAMIC AND GEOCHEMICAL ASSESSMENT OF THREE SUCCESSIVE CUTOFF MEANDERS OF THE DANUBE DELTA

*Laura DUŢU *, Dan SECRIERU *,*
*Florin DUŢU *, Irina CATIANIS ** and *Dan VASILIU **

* National Institute for Research and Development on Marine Geology and Geo-Ecology – GEOECOMAR, Dimitrie Onciul Street 23-25, Romania, laura.dutu@geoecomar.ro, ORCID: 0000-0003-3482-6938, dsecrieru@yahoo.com, ORCID:0000-0002-0931-8440, florin.dutu@geoecomar.ro, ORCID: 0000-0002-5393-3125, irina.catianis@geoecomar.ro, ORCID: 0000-0001-8120-736, dan.vasiliu@geoecomar.ro, ORCID: 0000-0002-5899-949X.

DOI: 10.2478/trser-2022-0008

KEYWORDS: Danube Delta, cutoff meander, sediment pollutants, sediment quality.

ABSTRACT

Hydrological and sedimentological data were collected on several cross-sections of both natural and artificial canals of three cutoff meanders (Mahmudia, Dunavăţul de Sus, and Dunavăţul de Jos meanders) of the Sfântu Gheorghe branch at the beginning of June 2017. The hydrological data shows a heterogeneous distribution of water discharges: on the meanders of Mahmudia and Dunavăţul de Jos, most of the liquid flow passes through artificial channels. In the case of the Dunavăţul de Sus meander, the cut meander is the main transport channel for the liquid flow. The statistical analysis of chemical data evidenced an excellent quality of the bottom sediments, with few parameters exceeding the limits (for Ni, Cu, and Cr). These results correlated with the hydrological measurements made on each investigated cross-section.

RÉSUMÉ: Evaluation hydrodynamique et géochimique de trois méandres recoupés du Delta du Danube.

Des données hydrologiques et sédimentologiques ont été collectées sur plusieurs sections transversales de chaneaux naturels et artificiels de trois méandres recoupées (méandres de Mahmudia, Dunavăţul de Sus et Dunavăţul de Jos) du bras de Sfântu Gheorghe au début du mois de Juin 2017. Les données hydrologiques montrent une distribution hétérogène des débits d'eau: sur les méandres de Mahmudia et Dunavăţul de Jos, la majeure partie du débit liquide passe par des canaux artificiels. Dans le cas du méandre de Dunavăţul de Sus, le méandre recoupé est le principal canal de transport du flux liquide. L'analyse statistique des données chimiques a mis en évidence une bonne qualité des sédiments de fond, avec peu de paramètres dépassant les limites (pour Ni, Cu et Cr).

REZUMAT: Evaluarea hidrodinamică şi geochimică a trei meandre succesive din delta Dunării.

Date hidrologice şi sedimentologice au fost colectate pe secţiuni transversale situate atât pe canalele naturale cât şi pe cele artificiale ale celor trei meandre ale braţului Sfântu Gheorghe la începutul lui iunie 2017 (meandrele Mahmudia, Dunavăţul de Sus şi Dunavăţul de jos). Datele hidrologice arată o distribuţie heterogenă a debitului de apă: pe meandrele Mahmudia şi Dunavăţul de Jos, cea mai mare parte a debitului trece prin canale artificiale. În cazul meandrului Dunavăţul de Sus, meandrul rectificat este principalul canal de transport pentru debitul lichid. Analiza statistică a datelor geochimice a evidenţiat o bună calitate a sedimentelor de fund, cu câţiva parametri care depăşesc limitele admise (pentru Ni, Cu şi Cr). Rezultatele au fost corelate cu măsurătorile hidrologice de pe fiecare secţiune transversală.

INTRODUCTION

The geochemistry of the bottom sediments is often affected by the chemical composition of their source rocks (Amorosi and Sammartino, 2007), by the anthropogenic influences, such as industrial cities, the presence of reservoirs (Sedlácek et al., 2013; Bábek et al., 2015), hydro-technical works on the channel planform (e.g., groins, embankments, jetties, meander cutoff) (Vasiliu et al., 2021) or by the interaction between tectonics and climate (Singh et al., 2016). These pressures produce the segmentation or even interruption of the sedimentary flow downstream (Tiron Duţu et al., 2019).

Extensive characterization of bed sediments along the whole course of the Danube River was carried out in 2001 and 2007 by the International Commission for the Protection of the Danube River (ICPDR) (Woitke et al., 2003; ICPDR, 2008). Other studies with a more detailed resolution and examining pollution by trace elements in the Danube Delta were performed by Secrieru and Secrieru (1996), Vignati et al. (2003), Oaie et al. (2005, 2015), Catianis et al. (2018), Tiron Duţu et al. (2019), and Vasiliu et al. (2021).

The Danube Delta begins at Ceatal Izmail (bifurcation), at Mile 44 from the river mouth, where the Danube divides into two branches: Chilia (going to the North) and Tulcea (going to the South). At Mile 34, the Tulcea Branch is further divided into the Sulina Branch to the North and Sfântu Gheorghe Branch to the South (Fig. 1) (Panin, 2003).

The Sfântu Gheorghe distributary starts at the hydrographic knot at Sfântu Gheorghe Ceatal (km 108.8 from the Black Sea). A major fault system (called the Sfântu Gheorghe fracture zone) at the north border of the North Dobrogean orogenic unit controls the general orientation of the distributary. The North Dobrogean unit represents a hard to erode "wall" that influences the river physiography. It results in the course of the Sfântu Gheorghe Branch subdividing into three sections (Panin, 1976): the Dobrogean section of limited meandering (between km 104 and km 90), the free, meandering segment (between km 90 and km 22) with a succession of six meander loops, and the downstream section of limited meandering (between km 22 and km 0). The Sfântu Gheorghe meander loops were rectified between 1984-1988, leading to a shortening of the distributary by about 31 km. As a result, the Sfântu Gheorghe distributary water and sediment discharges have slowly increased, reaching 26.5% of the water flow and suspended sediment discharge of the Danube River (Panin, 2003; Oaie et al., 2015; Tiron Duțu et al., 2019).

This paper further analyses previously published datasets, by the authors (Duțu et al., 2021), in relationship with the hydrological context of the study area.

MATERIAL AND METHODS

Study area

The survey was undertaken in June 2017 on the Sfântu Gheorghe distributary, the southern branch of the Danube within its Delta (Fig. 1). Three cutoff meanders represent the study area: Mahmudia, Dunavăţul de Sus, and Dunavăţul de Jos named here as M1, M2, and M3, respectively.

The period during which the measurements were made (1-2 June 2017) corresponds to average to high waters. The flow rate entering the study area (on profile A1) was 2,170 m^3/s^{-1} (Fig. 1). During the two days of measurements, the water flow discharge remained constant.

Hydrodynamic data were measured using a powered boat-mounted acoustic Doppler current profiler (Acoustic Doppler Current Profiler – ADCP, RiverRay 600 kHz, from Teledyne). 14 ADCP profiles were measured (Fig. 1).

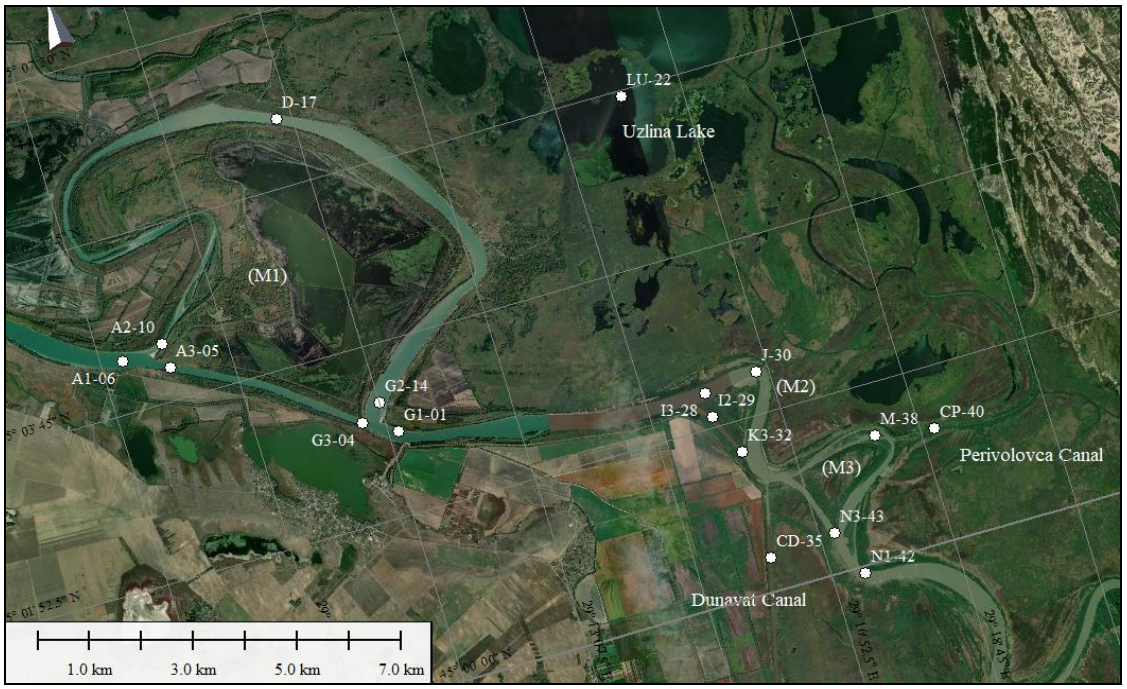

Figure 1: Map of the investigated area with the investigated cross-sections.

Based on the measured parameters such as maximum water depth, water velocity, and discharge, other specific hydrodynamical parameters were calculated, such as specific stream power (ω), mean bed shear stress (τ_0), water slope energy (S), for an overall estimation of water dynamic (Bravard and Petit, 1997; Duțu et al., 2018).

Bed sediment samples (17 samples) were collected from the main channel of the Sfântu Gheorghe Branch (14 samples collected from the center of the channel), from two lateral canals, Perivolovca Canal (one sample) and Dunavăț Canal (one sample), and the Uzlina Lake (one sample) (Fig. 1).

Geochemical analyses used the analytical procedures Secrieru and Secrieru (2002) described in detail. The analyses determined the concentrations of some major components – $CaCO_3$, TOC, Fe_2O_3, and minor ones – TiO_2 and MnO, which exercise significant control over the concentrations of trace elements. Some trace elements with genetic significance – Rb, Sr, Zr or toxic and potentially affected by anthropic influences – Cu, Pb, Zn, Cd, Cr, V, Ni, Co. Volumetric methods were used for analyzing $CaCO_3$ (Black, 1965) and TOC (total organic carbon), (Gaudette et al., 1974). Fe_2O_3 (total), TiO_2, Rb, Sr, Zr, and V have been analyzed by X-ray fluorescence spectroscopy using a VRA-30 sequential spectrometer on compacted powders; Mn, Co, Ni, Cu, Zn, Cr, and Pb have been determined by flame AAS and Cd – by graphite furnace AAS on an ATI UNICAM 939E AA spectrometer, after digestion of the samples with boiling HNO_3.

The accuracy and precision of AAS and XRF analyses were checked with several SRMs from US Geological Survey, NIST, and IAEA. Recovery for AAS varied from 93.2% (Co) to 99.4% (Pb), while for XRF the recovery range was from 90.3% (Zr) to 104.4% (Sr). Precision, expressed as the coefficient of variation for six replicate determinations varied for FAAS between 0.8% (Zn) and 4.5% (Mn); for XRF from 0.2% (Fe_2O_3) to 8.5% (V), the highest variability has been recorded for Cd – 12.5%, GFAAS determination.

RESULTS AND DISCUSSION

The water flux distribution between the natural course of meanders and cutoff canals varies from one sector to another, depending on several factors such as the ratio between the former and the new canal length, the diversion angle, and the bed level difference between the natural channel and the cutoff canal (Tiron Duțu et al., 2014).

The cutoff channel of M1 receives 3.8% of the upstream flow (Fig. 2; Tab. 1). The water discharge decreases progressively along the natural course of the meander, as well as the flow velocities (from 0.44 to 0.05 m/s^{-1}) (Fig. 3; Tab. 1). On the M2, the upstream discharge captured by the natural meander course was over 77.7% (Fig. 2).

The water flow acceleration in the natural channel shows the presence of incision processes at the bifurcation sector (I1-I2) with high-velocity values located in the right bank of the I2 profile (Fig. 3). The water fluxes at the bifurcation are distributed unequally between the natural course of the M3 meander (78 m^3/s^{-1}) and the cutoff canal (2003 m^3/s^{-1}), with a very high flux in the cutoff canal (≈96-97% of total) (Fig. 2). Local morphodynamical processes of the 2006 flood were analyzed through two geomorphological parameters: the specific stream power, indicating the stream's ability to adjust its channel morphology (Biedenharn et al., 2000); and the boundary shear stress indicating flow capacity to mobilize sediment from the bed as suspended-load or bedload.

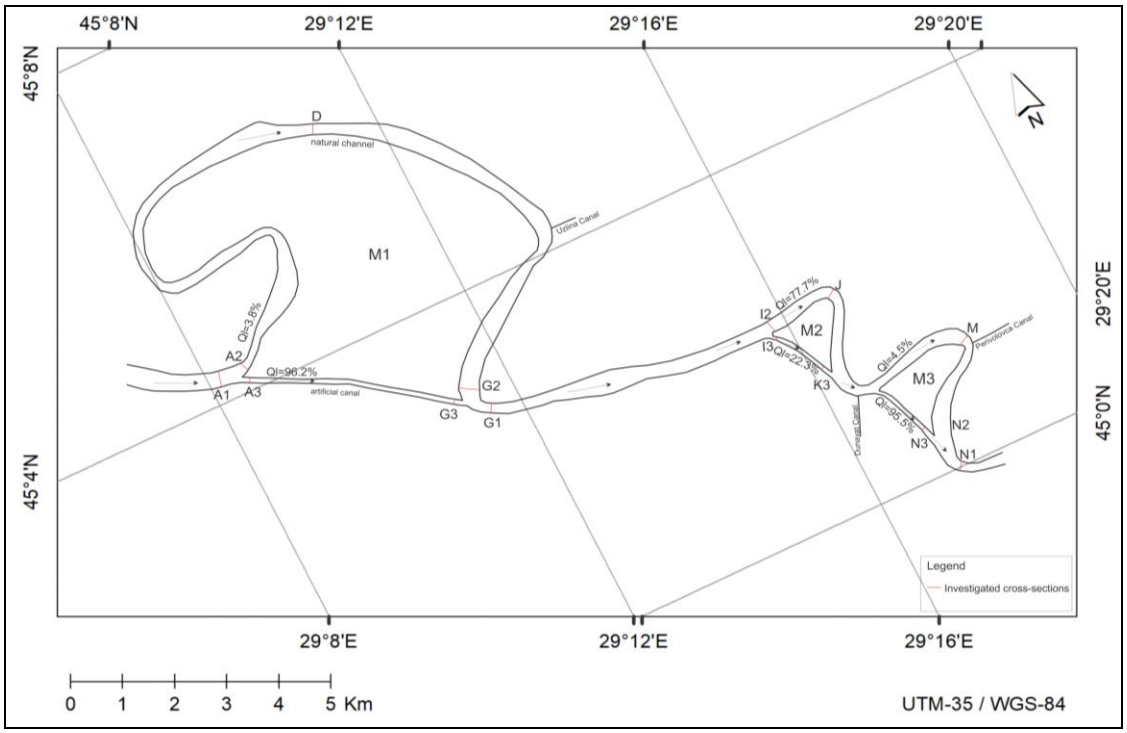

Figure 2: Water discharge repartition between the natural channel and artificial canals along the three investigated cutoff meanders.

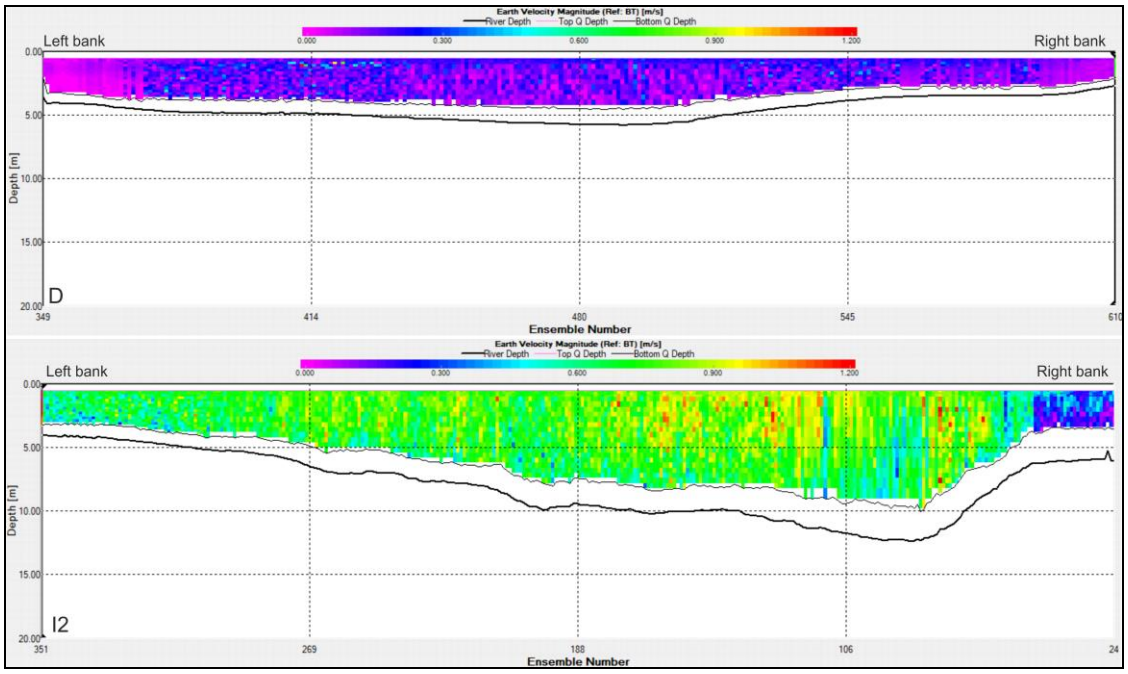

Figure 3: Velocities' magnitude distribution on the former meanders M1 and M2.

Morphodynamical activity is generally assessed by the specific stream power (ω) as an indicator of the river transport capacity (Bagnold, 1966):

$$\omega = \Omega / B \qquad [W.m^{-2}]$$

where *B* is the bankful channel width and Ω is the stream power that writes as:

$$\Omega = \rho\, g\, Q\, S \qquad [W.m^{-1}]$$

where the representative discharge *Q* [$m^3.s^{-1}$] is usually taken as the bankful discharge Q_{bf}.

Sectors with high specific stream power (above 4.00 $W.m^{-2}$) are found on the artificial canals (A3, I3, K3, and N3) and the main channel (A1 and G1). Along the former meanders, stream power values are much lower on M1 and M3 because of the lower slope and longer length (between 0.06 and 0.92 $W.m^{-2}$) and higher on M2 (1.2 $W.m^{-2}$) (Tab. 1).

The mean bed shear stress (τ_0) corresponds to the unit tractive force exerted on the bed:

$$\tau_0 = \rho\, g\, R\, S \qquad [N.m^{-2}]$$

Where ρ is the fluid density (1000 $kg.m^{-3}$ for sediment-free water), *g* is the gravitational acceleration (9.81 $m.s^{-2}$), *R* is the hydraulic radius [m], and *S* is the water-energy slope [$m.m^{-1}$].

The mean bed shear stress (τ_0) generally agrees with the stream power values. The shear stress is significantly higher along the main channel (A1, G1, and N1) (Tab. 1). In the former meander, shear stress values are dramatically lower (between 0.02 and 0.67 $N.m^{-2}$ on the profiles A2, G2, and M). The results offer a more continuous view of the complex variability of the hydrodynamic processes along the study reaches.

Chemical characteristics of the sediments

From a chemical point of view, the analyzed sediments can be classified based on their concentration of calcium carbonate as follows: terrigenous non-carbonated sediments – $CaCO_3 \leq 10\%$, weakly calcareous – $10\% < CaCO_3 \leq 30\%$, and calcareous sediments – $30\% < CaCO_3 \leq 50\%$.

Table 1: Location of the cross-sections and sediment samples, site description, and measured and calculated hydraulic parameters.

Profile/ sample	Site description	Depth (m)	Q water ($m^3.s^{-1}$)	Velocity ($m.s^{-1}$)	τ_0 ($N.m^{-2}$)	Ω ($W.m^{-2}$)
A1-06	Upstream bifurcation of M1	10.1	2170	0.85	5.25	4.95
A2-10	Downstream bifurcation of M1	1.5	85.1	0.1	0.14	0.13
A3-05	Artificial canal at the M1 bifurcation	17.4	2063	0.96	5.58	5.96
D-17	M1 natural course	4.5	82.4	0.1	0.10	0.06
G1-01	Downstream M1 confluence	8.8	2130.8	0.78	4.63	6.15
G2-14	Upstream M1 confluence	2.3	70.93	0.05	0.03	0.02
G3-04	Artificial canal at the M1 confluence	20.4	2068.3	0.78	3.49	2.93
I2-29	Downstream bifurcation on M2	9	1643.2	0.7	3.70	2.91
I3-28	Downstream bifurcation on M2 canal	4.4	465.2	0.68	4.43	9.72
J-30	Apex of M2	15.8	1705.1	0.55	1.89	1.20
K3-32	Upstream confluence on M2 canal	7.8	484.5	0.92	6.70	10.19
M-38	M2 natural course	3.1	83.4	0.25	0.67	0.92
N1-42	Downstream confluence of M3	12.5	2052.3	0.79	4.22	4.40
N3-43	Upstream confluence of M3 canal	21.8	1983.9	1.13	7.17	6.87
LU-22	Uzlina Lake	1.0	–	–	–	–
CD-35	Dunavăț Canal	5.6	–	–	–	–
CP-40	Perivolovca Canal	3.0	–	–	–	–

The geochemical characteristics of the sediments

The results of the geochemical analyses are given in tables 2a and 2b. The statistical analysis of the data (Tab. 3) evidenced a high compositional variability, with concentration variation coefficients ranging between 12.9% – Sr and 138.3% – TOC (Total Organic Carbon). From this point of view, the chemically analyzed compounds can be divided into two major groups: group I includes compounds with variability ranging from small to moderately high ($15\% < c_v < 50\%$), and group II, which includes compounds with high variability ($c_v > 50\%$).

Group I includes major compounds ($CaCO_3$, Fe_2O_3), minor compounds (TiO_2), and trace elements (Sr, Rb, V, and Co), with the variation coefficients ranging between 12.9% – Sr and 48.7% – Zr.

It is essential to underline the extremely low variability of the Sr, probably due to the presence of calcium carbonate in the form of calcite, a crystalline form in which Sr cannot replace calcium. Similarly, the variability of the $CaCO_3$ (c_v = 30.6%) concentrations are determined by the exceptional concentration ($CaCO_3 \approx 21.2\%$) in sample LU-22, characterized by the presence of shell fragments and whole shells of *Anodonta*. The elimination of value causes a decrease in the coefficient of variation to 18.6% and a slight reduction of the mean and median concentrations (Tab. 3a). For Zr, the variability of concentrations is determined by its exclusive presence in the form of zircon, whose sedimentation depends on the hydrodynamic environmental factors, which determine the concentration of the mineral in accumulations of heavy minerals, characteristic of coarse sediments.

The II-nd group includes compounds whose variation coefficients range between 50.6% – Co and 138.3% – TOC. Aside from the two components, the group consists of MnO (minor component) and the other determining trace elements. These high variabilities can have different causes. The highest variability recorded by TOC is determined by the biogenic origin of the TOC (especially in the primary productivity), combined with its chemical instability and the dependence of its concentration on its conservation in sediments. TOC preservation depends on sediment granulometry (fine particles much better preserve organic matter) and local physicochemical conditions (dissolved oxygen concentration). High concentrations of total organic carbon (TOC > 0.5%) characterize samples from fine silty sediments with low permeability. Exceptional concentrations (TOC > 1%), found in samples D-17 – 1.15% and especially LU2-22 – 2.6% TOC, are associated with the presence in sediments of easily oxidizable vegetal residues.

Mn is an element with extremely high redox sensitivity. The local physicochemical conditions can determine post-depositional processes that significantly affect the MnO concentrations in the sediments, leading to the increase of its variability.

In the case of heavy metals with high technophilic indices – Cu, Pb, and Cd, it is assumed that the anthropic contributions play a significant part in determining the variability of their concentrations.

As for the frequencies of the appearance of the concentrations of the analyzed compounds, their distribution curves show right-side asymmetries (Sk = 0.460-3.474). $CaCO_3$, TOC, and Sr have strongly leptokurtic distribution curves (K > 5), indicating the concentration values in a very narrow range. Cr, Pb, Cu, and Cd also have leptokurtic distribution curves, but kurtosis values range from 0.312 (Cu) to 1,345 (Cr). The curves are slightly platykurtic for all other components, with kurtosis values between –1,426 (TiO_2) and –0.052 (V).

Based on the values of these two parameters, the distribution curves of Fe_2O_3, TiO_2, MnO, Zr, Rb, Ni, V, and Co are considered normal, symmetrical, and mesokurtik. Important asymmetries (1,500 < K > 1,000) recorded for Zn, Cr, Pb, Cu, and Cd, do not allow the acceptance of the normality of their concentration distribution curves. The Shapiro-Wilk test also confirmed the normality of the TiO_2, V, and Co distributions for a probability $p > 0.05$. The same test confirms the normality of the distributions at a probability of $0.01 < p < 0.05$ for Fe_2O_3, Zr, Rb, and Ni, rejects the normality of the MnO distribution ($p = 0.0085$) and, instead, allows the acceptance of the normality of the Cr distribution ($p = 0.034$).

Generally, the chemically analyzed compounds can be divided into two major categories: biogenic compounds – $CaCO_3$, Sr, and TOC, and terrigenous compounds – the rest of the compounds. $CaCO_3$, a generally inferior compound in trace elements, Sr excepted, usually acts as a diluter for the terrigenous compounds. Given the relatively small variability in calcium carbonate concentrations, its role as a diluent in determining the variability in the concentrations of terrigenous compounds is minor. Under these circumstances, the determining role played by the hydrodynamic conditions that determine the gravitational particle differentiation of the sedimentary material.

Table 2a: Geochemical analyses on bed sediments of the three studied meanders during the field campaign from June 2017 to estimate the geochemical properties of bottom sediments and characterize the variation of major and trace elements.

Sample	$CaCO_3$, %	TOC, %	Fe_2O_3, %	TIO_2, %	Zr, µG/G	Sr, µG/G	RB, µG/G	Zn, µG/G
G1-01	7.22	0.07	2.30	0.48	98	185	55	24.54
G3-04	8.23	0.04	2.80	0.59	112	186	53	20.83
A3-05	11.41	0.02	2.60	0.42	92	199	48	26.07
A1-06	7.66	0.05	2.44	0.51	94	189	51	18.81
A2-10	10.64	0.07	2.73	1.13	192	190	47	19.22
G2-14	10.16	0.95	6.09	0.98	272	196	109	103.40
D-17	9.67	1.15	7.54	1.01	187	185	134	151.10
LU-22	21.18	2.60	5.18	0.45	103	290	91	119.10
I3-28	9.14	0.01	3.17	0.93	117	176	37	16.12
I2-29	8.96	0.06	2.83	0.63	99	187	49	21.88
J-30	12.13	0.24	4.11	0.80	292	194	75	37.78
K3-32	13.20	0.72	6.01	1.02	285	183	104	73.82
CD2-35	12.13	0.53	5.34	0.93	347	210	106	74.98
M-38	10.20	0.06	2.65	0.71	143	203	54	23.47
CP2-40	10.52	0.86	5.61	0.95	316	190	103	96.26
N1-42	6.95	0.06	2.34	0.62	137	191	54	19.90
N3-43	11.38	0.72	5.84	0.83	244	189	105	68.63

Table 2b: Results of geochemical analyses on bed sediments of the three studied meanders during the field campaign from June 2017 to estimate the geochemical properties of bottom sediments and characterize the variation of major and trace elements.

Sample	Ni, µg/g	MnO, %	Cr, µg/g corr	V, µg/g	Co, µg/g	Pb, µg/g	Cu, µg/g	MnO, %	Cd, µg/g
G1-01	23.9	0.024	31.5	46	6.83	9.717	4.367	0.024	0.07
G3-04	18.1	0.021	30.4	44	4.64	8.762	3.86	0.021	0.071
A3-05	23.0	0.033	31.7	66	7.38	10.81	4.211	0.033	0.073
A1-06	17.7	0.019	28.6	43	3.88	9.019	2.934	0.019	0.056
A2-10	14.9	0.021	14.0	77	3.25	8.62	4.064	0.021	0.064
G2-14	50.7	0.107	89.7	114	12.60	24.2	44.84	0.107	0.296
D-17	73.9	0.111	127.0	144	16.28	38.18	69.80	0.111	0.427
LU-22	51.4	0.133	55.6	64	11.81	38.06	69.62	0.133	0.571
I3-28	14.0	0.019	19.2	89	3.31	7.529	3.00	0.019	0.048
I2-29	19.5	0.020	18.0	43	5.46	7.968	3.02	0.020	0.079
J-30	28.2	0.050	48.4	64	6.44	11.8	11.01	0.050	0.125
K3-32	51.8	0.090	75.2	88	12.37	22.52	26.37	0.090	0.182
CD2-35	42.9	0.069	57.7	110	11.24	16.68	28.75	0.069	0.281
M-38	18.8	0.015	19.4	69	4.68	8.368	4.21	0.015	0.079
CP2-40	46.2	0.085	70.7	99	10.87	20.44	41.81	0.085	0.325
N1-42	17.8	0.020	22.1	76	4.09	8.585	3.64	0.020	0.058
N3-43	51.5	0.075	59.9	104	11.59	20.35	27.37	0.075	0.177

Table 3a: Descriptive statistics for the concentrations of the studied variables of the collected sediment samples.

Sample	$CaCO_3$, %	TOC, %	Fe_2O_3, %	TiO_2, %	Zr, µg/g	Sr, µg/g	Rb, µg/g	Zn, µg/g
Mean	10.63	0.48	4.09	0.76	184.11	196.64	75	53.87
Median	10.2	0.07	3.17	0.8	143	190	55	26.07
Standard Deviation	3.25	0.66	1.71	0.22	89.64	25.34	29.95	42.54
Minimum	6.95	0.01	2.3	0.42	92	176	37	16.12
Maximum	21.18	2.60	7.54	1.13	347	290	134	151.1
Cv, %	30.62	138.28	41.85	29.91	48.69	12.89	39.94	78.97
Count	17	17	17	17	17	17	17	17

Table 3b: Descriptive statistics for the concentrations of the studied variables of the collected sediment samples.

Sample	Ni, µg/g	MnO, %	Cr, µg/g corr	V, µg/g	Co, µg/g	Pb, µg/g	Cu, µg/g	Cd, µg/g
Mean	33.19	0.05	47.00	78.82	8.042	15.97	20.75	0.17
Median	23.86	0.032	31.73	76	6.82	10.81	4.36	0.07
Standard Deviation	18.13	0.03	30.72	28.78	4.06	10.05	23.27	0.15
Minimum	13.98	0.01	13.95	43	3.248	7.52	2.93	0.04
Maximum	73.92	0.13	126.95	144	16.28	38.18	69.8	0.57
Cv, %	54.63	73.71	65.37	36.51	50.58	62.91	112.15	87.65
Count	17	17	17	17	17	17	17	17

Geochemical relations between components

Sediments result from mixing between the terrigenous material, biogenic calcium carbonate (generally low in heavy metals), and a low quantity of organic matter (Dutu et al., 2019). Due to this mixing process, a number of relationships are established between the chemical compounds, which are frequently linear and are identified by calculating the linear correlation coefficients (Tab. 4).

The analysis of the matrix of the linear correlation coefficients (Tab. 4) clearly emphasizes the complete lack of calcium carbonate dilution effect for these analyzed samples. Moreover, $CaCO_3$ correlates positively with the vast majority of terrigenous compounds (except TiO_2), in some cases significant at the critical statistical confidence level $\alpha = 0.05$ – Zn, Pb, Cu, and Cd. The significant association of calcium carbonate with these heavy metals can only be explained by the abiogenic origin of a considerable amount of calcium carbonate, most likely resulting from the surface alteration of complex sulfide mineralizations, in which calcium carbonate, generally present as calcite, appears as a secondary mineral.

A fascinating aspect revealed by the matrix of linear correlation coefficients (Tab. 4) is the close association of TOC with the vast majority of terrigenous compounds, especially with Zn, Pb, Cu, and especially Cd. The linear correlation coefficients of TOC with these metals have a statistical significance higher than those of Fe_2O_3 or Rb, with which metals are usually associated.

Table 4a: Correlation matrix (Pearson) for the major constituents, minor constituents and heavy metals ($r_{17;\ 0.05;\ 95} = 0.482$).

Compound	$CaCO_3$ %	TOC %	Fe_2O_3 %	TiO_2 %	Zr µg/g	Sr µg/g	Rb µg/g	Zn µg/g
$CaCO_3$, %	1							
TOC, %	**0.817**	1						
Fe_2O_3, %	0.434	**0.689**	1					
TiO_2, %	– 0.021	0.051	**0.567**	1				
Zr, µg/g	0.191	0.200	**0.666**	**0.714**	1			
Sr, µg/g	**0.854**	**0.779**	0.161	– 0.359	– 0.112	1		
Rb, µg/g	0.381	**0.668**	**0.969**	0.480	**0.691**	0.180	1	
Zn, µg/g	**0.517**	**0.841**	**0.926**	0.356	0.459	0.394	**0.923**	1
Ni, µg/g	0.457	**0.753**	**0.965**	0.385	**0.529**	0.257	**0.970**	**0.960**
MnO, %	**0.675**	**0.906**	**0.907**	0.303	**0.489**	**0.506**	**0.889**	**0.956**
Cr, µg/g	0.262	**0.610**	**0.938**	0.445	**0.542**	0.068	**0.942**	**0.922**
V, µg/g	0.120	0.378	**0.823**	**0.725**	**0.622**	– 0.091	**0.786**	**0.733**
Co, µg/g	0.458	**0.725**	**0.939**	0.333	**0.531**	0.261	**0.956**	**0.939**
Pb, µg/g	**0.637**	**0.917**	**0.858**	0.220	0.290	**0.528**	**0.841**	**0.964**
Cu, µg/g	**0.605**	**0.914**	**0.870**	0.272	0.362	**0.524**	**0.858**	**0.984**
Cd, µg/g	**0.707**	**0.950**	**0.788**	0.170	0.334	**0.669**	**0.787**	**0.937**

Table 4b: Correlation matrix (Pearson) for the major constituents, minor constituents and heavy metals ($r_{17;\ 0.05;\ 95} = 0.482$).

Compound	Ni µg/g	MnO %	Cr µg/g corr	V µg/g	Co µg/g	Pb µg/g	Cu µg/g	Cd µg/g
$CaCO_3$, %								
TOC, %								
Fe_2O_3, %								
TiO_2, %								
Zr, µg/g								
Sr, µg/g								
Rb, µg/g								
Zn, µg/g								
Ni, µg/g	1							
MnO, %	**0.931**	1						
Cr, µg/g	**0.951**	**0.857**	1					
V, µg/g	**0.755**	**0.632**	**0.782**	1				
Co, µg/g	**0.985**	**0.920**	**0.935**	**0.728**	1			
Pb, µg/g	**0.924**	**0.955**	**0.849**	**0.613**	**0.893**	1		
Cu, µg/g	**0.915**	**0.958**	**0.851**	**0.656**	**0.886**	**0.981**	1	
Cd, µg/g	**0.838**	**0.932**	**0.744**	**0.540**	**0.821**	**0.945**	**0.975**	1

The close association is partly explained by the preferential concentration of organic matter in the fine sediments, which allow its preservation and in which the terrigenous compounds are also concentrated. However, this cannot fully explain the extremely high statistical significance of TOC-metal relationships, which suggests that at least some of the metals contained in sediments come from bioavailable forms and reach sediments through organic matter in the form of organo-metallic compounds.

The same metals have the highest values of linear correlation coefficients with MnO, a probable consequence of both their association in the fine material and the adsorption capacities of hydrated manganese oxides, which concentrate metals in soluble forms.

Co, Ni, Cr, Cu, Pb, Zn, and Cd tightly correlate among each other and the Fe_2O_3 and Rb concentrations, indicating their association in the terrigenous material. The linear correlation coefficients of V with Fe_2O_3 and Rb have lower values ($r_{Fe\text{-}V}$ = 0.823 and $r_{Rb\text{-}V}$ = 0.786) due to the concentration of some V minerals in the accumulations deposits of heavy metals. This process leads to the partial alteration of its relations with the other two components. Due to their concentration in fine silicate fraction, the linear correlation coefficients between metals and Fe_2O_3 are relatively close to those with Rb.

Sediments quality

Order 161/2006 of the Romanian Ministry of Environment and Water Management sets quality criteria for many chemical compounds, organic and inorganic, in sediments; these include many heavy metals (Tab. 5). Comparing the mean concentrations of the primary metals (Tab. 4) with high toxicity to the criteria in effect in Romania (Tab. 5) proves that overall, at the level of the investigated area, these fit the criteria, indicating a good quality of the sediments.

However, the comparison between the criteria and the maximum values of the concentrations of the investigated metals show exceeding concentrations/ratios for Ni, Cr, and Cu. In the case of Ni and Cu, the exceeding concentrations/ratios are frequent: Ni – 41.2% and Cu – 23.5% of the analyzed samples. Cr and Zn exceed the quality criterion in a single sample (D-17).

Table 5: Quality criteria for several chemical compounds, organic and inorganic, in sediments (Order 161/2006).

Metal	UM	Ord. 161/2006	Mean concentration	Concentrations exceeding Ord. 161 criteria
Cadmium (Cd^{2+})	µg/g	0.8	0.175	0
Total chromium (Cr^{3+} + Cr^{6+})	µg/g	100	47	1
Copper (Cu^{2+})	µg/g	40	20.8	4
Lead (Pb^{2+})	µg/g	85	16	0
Zinc (Zn^{2+})	µg/g	150	53.9	1
Nickel (Ni^{2+})	µg/g	35	33.2	7

Still, the systematic exceeding of the quality criteria does not necessarily mean an intense pollution process, just as compliance with the quality criteria does not necessarily imply the absence of pollution. It needs to be taken into account that these criteria are general, set exclusively based on biological criteria, without considering the regional and local geochemical background.

The natural abundance of nickel in the Earth's crust, which through alteration generates sedimentary nickel, is 84 µg/g, more than twice the median concentration. The same applies to Cr, which has an abundance of 140 µg/g – almost three times more than the average concentration of Cr in the analyzed samples and Cu – an abundance of 55-60 µg/g, mean concentration of 21.8 µg/g.

One more argument favoring the normality of the concentrations of these metals is represented by the very close relationships between the concentrations of the incriminated metals and the concentrations of the non-technophilic chemical compounds Fe_2O_3 and Rb, relations with a very high degree of statistical significance. The linear regression analysis and the calculation of the prediction interval for the concentration of the heavy metal (the dependent variable) subject to the concentration of the independent variable (non-technophile compound) highlights, for instance, the case of the relationship Fe_2O_3 – Ni (Fig. 4), the fitting of the Ni concentrations within the prediction interval of the relationship:

$$C_{Ni} = 10.210*C_{Fe2O3} - 8.597,\ R^2 = 0.930$$

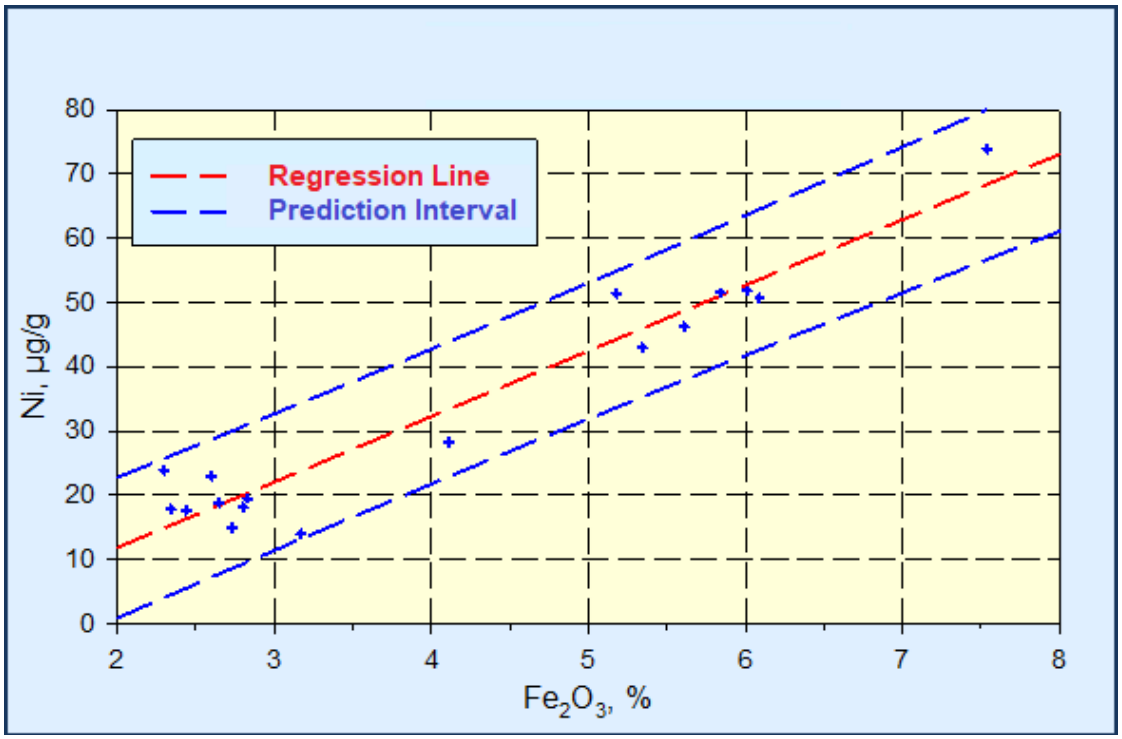

Figure 4: Linear regression diagram Fe_2O_3 – Ni,
with the prediction interval
($C_{Ni} = 10.210*C_{Fe2O3} - 8.597,\ R^2 = 0.930$)

They can be considered normal; their variation is determined by natural processes leading to either the dilution or the concentration of the nickel-bearing sedimentary material. A similar result was obtained for Cr and shows that only one sample exceeded the quality criterion (127 µg/g Cr, on D-17) but fits in the prediction interval of the relationship (Fig. 5):

$$C_{Cr} = 16.818*Fe_2O_3\text{-}21.831,\ R^2 = 0.879$$

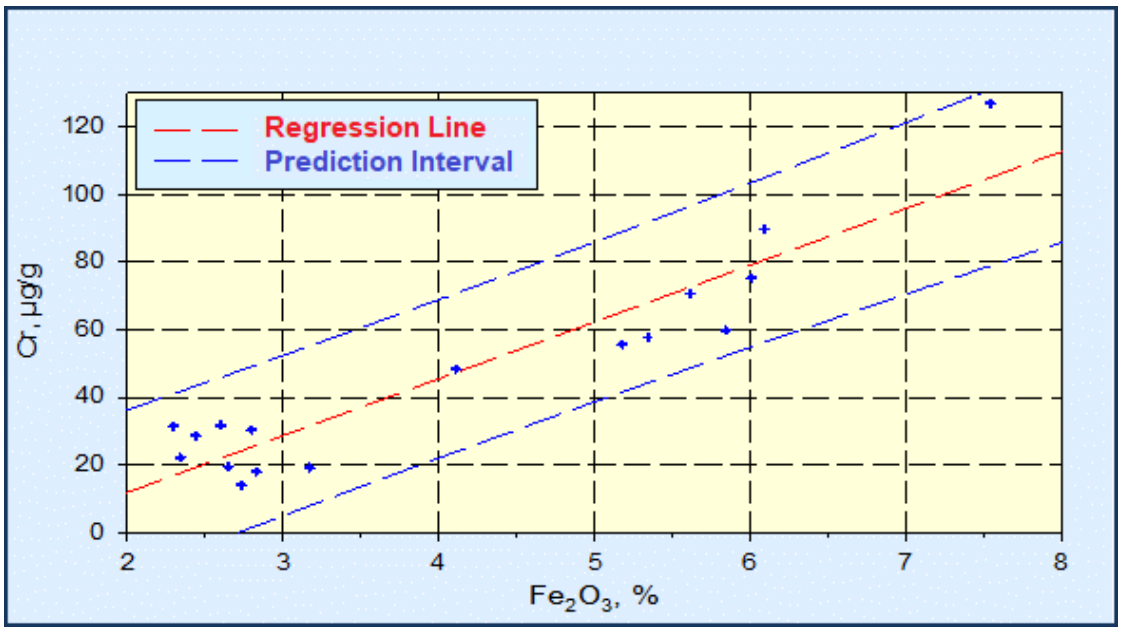

Figure 5: Linear regression diagram Fe_2O_3 – Cr,
with the prediction interval
($C_{Cr} = 16.818*Fe_2O_3\text{-}21.831,\ R^2 = 0.879$)

Also, for Zn, the concentration of 151.1 µg/g Zn in sample D-017 can be considered normal (Fig. 6). However, in this case, the analysis reveals that in the sample LU2-22, the Zn concentration, although lower than the quality criterion (C_{Zn} = 119.1 µg/g), is more than that predictable of the Fe_2O_3 – Zn relationship (Fig. 6). It indicates low Zn contributions of possible anthropic origin.

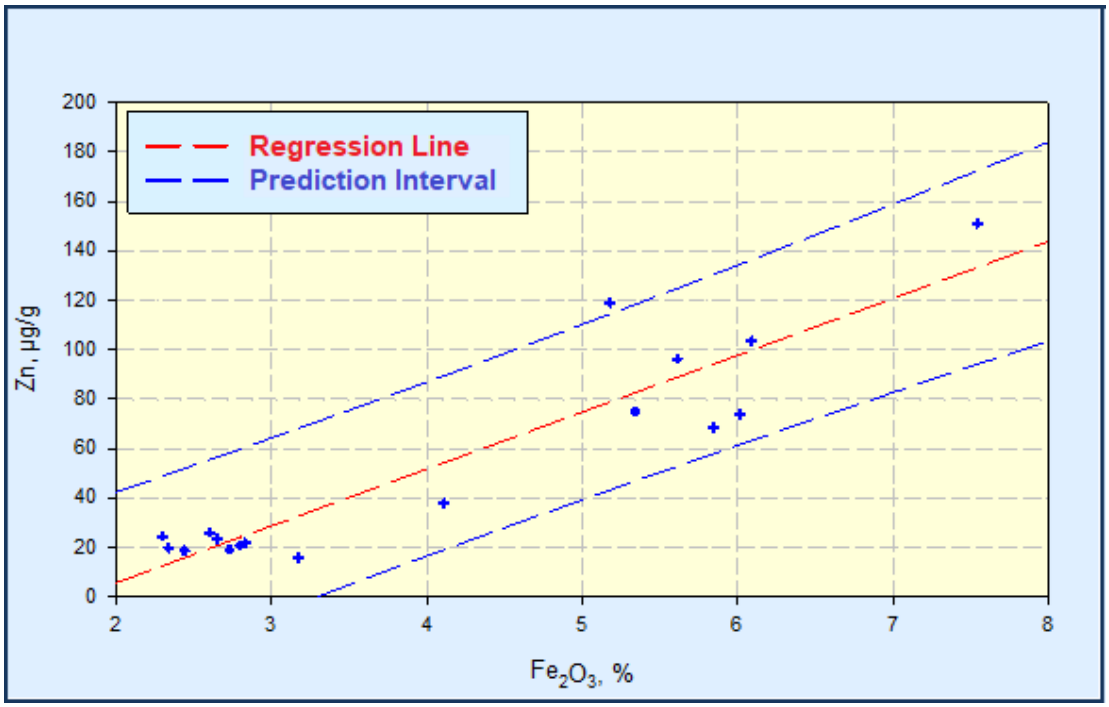

Figure 6: Linear regression diagram Fe_2O_3 – Zn,
with the prediction interval
(C_{Zn} = 23.007*C_{Fe2O3} –0.289, R^2 = 0.858).

In the case of Cu, the analysis reduced the number of abnormal concentrations from four to one, whose concentration exceeds the prediction interval of the relationship Fe_2O_3 – Cu – sample LU-22, Lake Uzlina – 69.6 µg/g Cu (Fig. 7). The excessive concentration of Cu in this sample is also accompanied by concentrations of Pb and Cd that exceed the limits of the prediction range, even if they are lower than the quality criteria, indicating possible influences of mining activities.

In previous considerations, it is concluded that the sediments in the investigated area comply qualitatively. The elevated concentrations of the heavy metals are, for the most part, the result of the sedimentary material originating from the Dobrudjan green schists characterized by high natural concentrations of Ni, Cu, and Cr. At the same time, the analyzes clearly show that compliance with the quality criteria does not exclude anthropogenic or natural contributions independent of the sedimentary material.

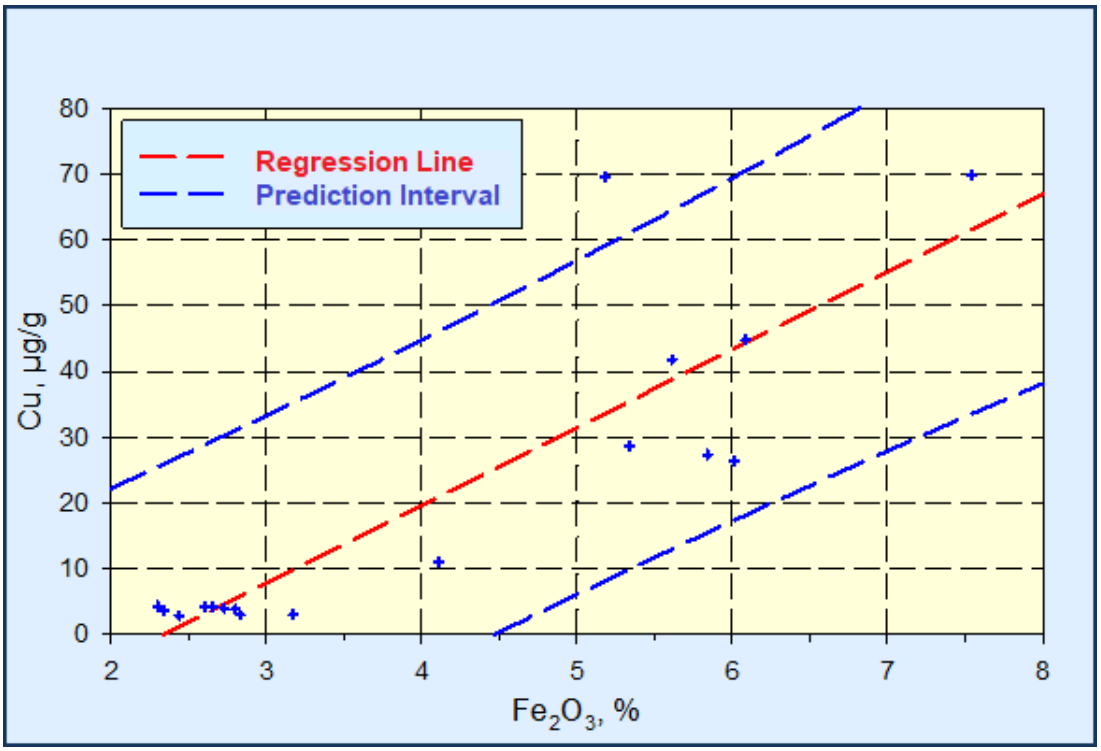

Figure 7: Linear regression diagram Fe_2O_3 – Cu, with the prediction interval ($C_{Cu} = 11.826*C_{Fe2O3} - 27.644$, $R^2 = 0.757$)

CONCLUSIONS

Generally, the highest concentrations of terrigenous compounds appear in the samples collected from the natural canals. Occasionally, high concentrations of these compounds are also encountered at the exits from the rectification canals on the Sfântu Gheorghe Branch (samples K3-32 and N3-43). It is expected that the hydrodynamic conditions, among which the speed of the current is probably the determining factor, will facilitate the accumulation of fine material (silt and clay). The terrigenous compounds are concentrated and favor the conservation of organic matter. In the other sectors, a more active hydrodynamic regime favors the deposition of coarse material (coarse silt and mainly sand), generally quartzitic, poor in terrigenous compounds and organic matter. The coarse sediments are often characterized by enrichment in heavy minerals, clearly evidenced by high concentrations of TiO_2, Zr, and sometimes V – especially the A1-08, A2-11, G1-01, I2-29, and CD-35 samples.

ACKNOWLEDGEMENTS

The research was supported by the Romanian Ministry of Research, Innovation and Digitization Core Program, Projects PN16450503 (Contract no. 37N/2016) and PN19200401 (Contract no. 13N/08.02.2019), and Project AMBIACVA (Contract 23PFE/30.12.2021).

REFERENCES

1. Amorosi A. and Sammartino I., 2007 – Influence of sediment provenance on background values of potentially toxic metals from near-surface sediments of Po coastal plain (Italy), *International Journal of Earth Sciences*, 96, 389-396.
2. Bábek O., Grygar T. M., Faměra M., Hron K., Nováková T. and Sedláček J., 2015 – Geochemical background in polluted river sediments: How to separate the effects of sediment provenance and grain size with statistical rigour? *Catena*, 135, 240-253.
3. Bagnold R. A., 1966 – An approach to the sediment transport problem from general physics, *U.S. Geological Survey*, 422, I, 1-37.
4. Biedenharn D. S., Thorne C. R. and Watson C. C., 2000 – Recent morphological evolution of the lower Mississippi River, *Geomorphology*, 34, 227-249.
5. Black C. A., 1965 – Methods of soil analysis, American Society of Agronomy, Monograph 9, Madison, Wisconsin, 1572.
6. Bravard J.-P. and Petit F., 1997 – Les cours d'eau, Dynamique du système fluvial, Paris, Armand Colin, Collection, 222. (in French)
7. Catianis I., Secrieru D., Pojar I., Grosu D., Scrieciu A., Pavel A. B. and Vasiliu D., 2018 – Water quality, sediment characteristics and benthic status of the Razim-Sinoie Lagoon system, Romania, *Open Geosciences*, 10, 12-33.
8. Duţu F., Panin N., Ion G. and Tiron Duţu L., 2018 – Multibeam bathymetric investigations of the morphology and associated bedforms, Sulina Channel, Danube Delta, *Geosciences*, 8, 1, 7, 1-17.
9. Duţu L., Secrieru D., Duţu F. and Lupaşcu N., 2021 – Geochemical dataset of the Danube Delta sediments, *Data in Brief*, 39, 107529.
10. Gaudette H. E., Flight W. R., Toner L. and Folger D. W., 1974 – An inexpensive titration method for the determination of organic carbon in recent sediments, *Journal of Sedimentary Research*, 44, 1, 249-53.
11. ICPDR, 2008 – Joint Danube Survey 2, Final Scientific Report, ICPDR, Vienna, 242.
12. Romanian Ministerial Order No 161/2006 for the Approval of the Norm Concerning the Reference Objectives for the Surface Water, Quality Classification (Including Quality Standards for Sediments).
13. Oaie G., Secrieru D., Szobotka S, Fulga C. and Stanică A., 2005 – River Danube: sedimentological, mineralogical and geochemical characteristics of the bottom sediments, *Geo-Eco-Marina*, 11-12, 77-85.
14. Oaie G., Secrieru D., Bondar C., Szobotka S., Duţu L., Stănescu I., Opreanu G., Duţu F., Pojar I. and Manta T., 2015 – Lower Danube River: characterization of sediments and pollutants, *Geo-Eco-Marina*, 21, 19-34.
15. Panin N., 1976 – Some aspects of fluvial and marine processes in Danube Delta, *Institutul de geologie şi geofizică, Anuarul Institutului Geologie şi Geofizică*, L, 149-165.
16. Panin N., 2003 – The Danube Delta, geomorphology and Holocene evolution: a synthesis, *Geomorphologie: relief, processus, environnement*, 4, 247-262.
17. Secrieru D. and Secrieru A., 1996 – Anthropic increases of trace element concentrations in sediments from the Black Sea Romanian shelf – Danube Delta-Black Sea system under global changes impact, *Geo-Eco-Marina*, 1, 93-98.
18. Secrieru D. and Secrieru A., 2002 – Heavy metal enrichment of man-made origin of superficial sediments of the continental shelf of the north-western Black Sea, *Estuarine, Coastal and Shelf Sciences*, 54, 513e526.
19. Sedlácek J., Bábek O. and Matys Grygar T., 2013 – Trends and evolution of contamination in a well-dated water reservoir sedimentary archive: the Brno Dam, Moravia, Czech Republic, *Environmental Earth Sciences*, 69, 2581-2593.

20. Singh A., Debajyoti P., Sinha R., Thomsen K. J. and Gupta S., 2016 – Geochemistry of buried river sediments from Ghaggar Plains, NW India: Multi-proxy records of variations in provenance, paleoclimate, and paleovegetation patterns in the Late Quaternary, *Palaeogeography, Palaeoclimatology, Palaeoecology*, 449, 85-100.
21. Tiron Duţu L., Provansal M., Le Coz J. and Duţu F., 2014 – Contrasted sediment processes and morphological adjustments in three successive cutoff meanders of the Danube Delta, *Geomorphology*, 204, 154-164.
22. Tiron Duţu L., Duţu F., Secrieru D. and Opreanu G., 2019 – Sediments grain size and geochemical interpretation of three successive cutoff meanders of the Danube Delta, Romania, *Geochemistry*, 79, 399-407.
23. Vasiliu D., Tiron Duţu L., Bucşe A., Lupaşcu N. and Duţu F., 2021 – Geochemical characteristics of riverbed sediments in the Danube Delta, Romania, *Scientific Papers, Series E., Land Reclamation, Earth Observation & Surveying, Environmental Engineering*, X, 258-264.
24. Vignati D., Pardos M., Diserens J., Ugazio G., Thomas R. and Dominik J., 2003 – Characterisation of bed sediments and suspension of the river Po (Italy) during normal and high flow conditions, *Water Research*, 37, 12, 2847e2864.
25. Woitke P., Wellmitz J., Helm D., Kube P., Lepom P. and Litheraty P., 2003 – Analysis and assessment of heavy metal pollution in suspended solids and sediments of the river Danube, *Chemosphere*, 51, 633e642.